

Intelligent Stabilization Control to An Arbitrary Equilibrium Point of Double Pendulum

Masaki Takahashi, Terumasa Narukawa and Kazuo Yoshida

Abstract—This study aims at establishing a robust and effective intelligent control method for nonlinear and complicated systems. In the method, an integrator neural network acquires suitable switching and integration of several controllers for a different local purpose by calculating the fitness function based on the system objective using the genetic algorithm. The proposed method is applied to an equilibrium point transfer and stabilization control of a double pendulum that possesses four equilibrium points. In order to verify the effectiveness of the proposed method, computational simulations and experiments using a real apparatus were carried out. As a result, it was demonstrated that the integrated intelligent controllers can transfer and stabilize the double pendulum from an arbitrary equilibrium point to a desired unstable equilibrium point without touching the cart position limit.

I. INTRODUCTION

In recent years, it has been desired to establish an effective control technique for nonlinear and complicated systems. In general, however, it is not easy to derive a nonlinear control law for nonlinear and complicated systems. For example, there are several equilibrium points in such system. Nonlinear systems may be regarded as a linear system in the vicinity of the equilibrium point and many effective linear control methods have been established. However, as for a nonlinear control such as a transfer control between equilibrium points, there have been few effective and systematic control design approaches widely applicable to such systems. This study aims at establishing a robust intelligent control method with higher control performance and wider applicable region for nonlinear system. The configuration of the proposed integrated intelligent control system is shown in Fig.1. In the system, an integrator neural network is prepared in parallel with several controllers for each different local purpose. The integrator switches and integrates several controllers autonomously and adequately based on the system states. It is expected that the proposed method enable us to accomplish several control purposes by using less controllers and switching laws. The integrator is specified by some parameters. In this study, the adjustment of these parameters is performed

M. Takahashi is with School of Science for Open and Environmental System Faculty of Science and Technology, Keio University, 3-14-1, Hiyoshi, Kohoku-ku, Yokohama 223-8522, JAPAN masaki55@2000.jukuin.keio.ac.jp

T. Narukawa is with School of Science for Open and Environmental System Faculty of Science and Technology, Keio University, 3-14-1, Hiyoshi, Kohoku-ku, Yokohama 223-8522, JAPAN narukawa@yoshida.sd.keio.ac.jp

K. Yoshida is with the Department of System Design Engineering, Keio University, 3-14-1 Hiyoshi, Kohoku-ku, Yokohama 223-8522, JAPAN yoshida@sd.keio.ac.jp

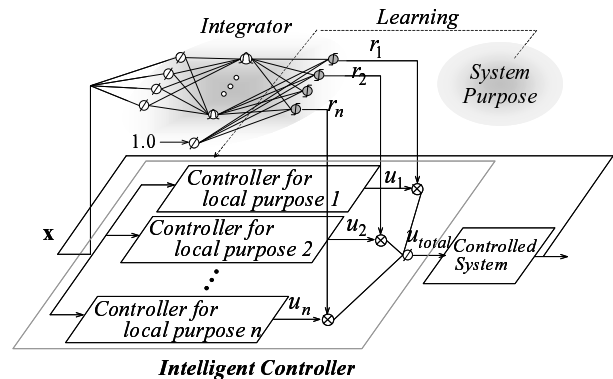


Fig. 1. Integrated Intelligent Control System.

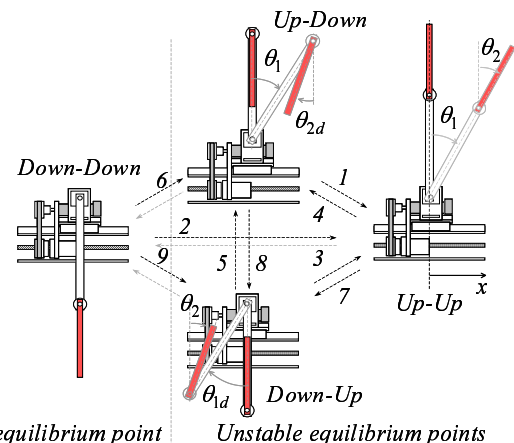


Fig. 2. Equilibrium Point Transfer and Stabilization Control Problem.

by a probabilistic optimization method utilizing evolution strategies such as the Genetic Algorithm (GA).

The proposed method is applied to an equilibrium point transfer and stabilization control of a double pendulum mounted on a cart. Since the double pendulum possesses a stable equilibrium point (Down-Down) and three unstable equilibrium points (Down-Up, Up-Down and Up-Up), there are nine paths between equilibrium points in this control problem as shown in Fig.2 [1]. To achieve these controls, both a transfer control from one equilibrium point to the other in nonlinear region and a stabilization control near the unstable equilibrium point in linear region are required. In this study, only one swing-up controller, three stabilization controllers and three integrator neural networks are designed to accomplish all nine paths from an arbitrary equilibrium point to the desired unstable equilibrium point. In order to verify the effectiveness of the proposed method, computational simulations and experiments are carried out by an experimental setup.

II. EQUILIBRIUM POINT TRANSFER AND STABILIZATION CONTROL

As a typical unstable nonlinear system, single inverted pendulum has been widely used to compare different control methods for dynamic systems [2]-[4]. Double or triple inverted pendulums have been used to verify the effectiveness of new control approach for dynamic systems with high-order nonlinearities [5]-[7]. This study deals with an equilibrium point transfer and stabilization control of the double pendulum from the arbitrary equilibrium point to the desired unstable equilibrium point. In the case that the available cart track length is unlimited, this control problem was studied in Yamakita and Furuta et al [1][8][9]. In order to accomplish these controls, a number of controllers and switching rules were prepared for each path so far. Twelve controllers and eleven switching rules were required to realize five paths, that is, path 1, 2, 4, 6 and 9 in Fig.2. In this study, since a cart and double pendulum system shown in Fig.3 is used, there is an inherent restriction on the cart track length and the magnitude of control force that can be applied. In addition, there are the various uncertainties such as friction, disturbance and so on. Therefore, the control problem dealt with in this study is how to design a robust controller for a strong nonlinear and complicated system of double pendulum to cope with the physical limitations and the influence of various uncertainties.

III. DOUBLE PENDULUM

The double pendulum on a cart is an under-actuated mechanical system with three degrees of freedom and one control input. The model of the system is shown in Fig.4. The cart is driven through the rotary nut which is rotated by the DC servo motor through timing belt. The pendulum 1 and the rotary encoder measuring the angle of the pendulum 1 are installed at the cart. The pendulum 2 is jointed at the pendulum 1 through the rotary encoder measuring the angle of pendulum 2 on the top of pendulum 1. Each pendulum is able to rotate freely in the vertical plane. The equations of motion of cart, pendulum 1 and pendulum 2 can be written as follows:

$$\begin{aligned} & (M_c + M_{p1} + M_{p2}) \ddot{x} \\ & + (M_{p1}L_1 + M_{p2}L_2 \cos(\theta_1 + \theta_2) + M_{p2}L_{p1} \cos\theta_1) \ddot{\theta}_1 \\ & + M_{p2}L_2 \cos(\theta_1 + \theta_2) \ddot{\theta}_2 + C_c \dot{x} = F - f_c \end{aligned} \quad (1)$$

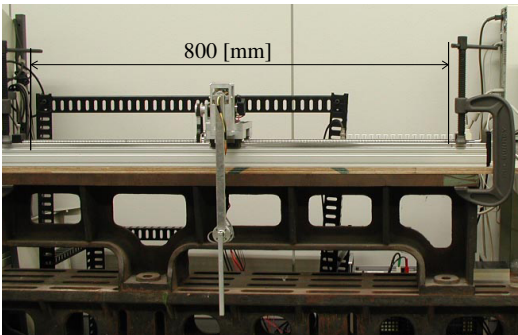


Fig. 3. Experimental Facility.

$$\begin{aligned} & (M_{p1}L_1 \cos\theta_1 + M_{p2}L_2 \cos(\theta_1 + \theta_2) + M_{p2}L_{p1} \cos\theta_1) \ddot{x} \\ & + (I_1 + I_2 + M_{p1}L_1^2 + M_{p2}L_2^2 + M_{p2}L_{p1}^2 + 2M_{p2}L_{p1}L_2 \cos\theta_2) \ddot{\theta}_1 \\ & + (I_2 + M_{p2}L_2^2 + M_{p2}L_{p1}L_2 \cos\theta_2) \ddot{\theta}_2 + C_p \dot{\theta}_1 - M_{p1}L_1 g \sin\theta_1 \\ & - M_{p2}g (L_{p1} \sin\theta_1 + L_2 \sin(\theta_1 + \theta_2)) \theta_1 = 0 \end{aligned} \quad (2)$$

$$\begin{aligned} & M_{p2}L_2 \cos(\theta_1 + \theta_2) \ddot{x} + (I_2 + M_{p2}L_2^2 + M_{p2}L_{p1}L_2 \cos\theta_2) \ddot{\theta}_1 \\ & + (I_2 + M_{p2}L_2^2) \ddot{\theta}_2 + C_p \dot{\theta}_2 + M_{p2}L_2 g \sin(\theta_1 + \theta_2) = 0 \end{aligned} \quad (3)$$

All symbols used in the above equations are defined in Fig.4. $x(t)$ is the displacement of the cart. $\theta_1(t)$ and $\theta_2(t)$ indicate the angle of the pendulum 1 and the angle of the pendulum 2 relative to the pendulum 1, measured positive in a clockwise direction respectively. Consider the translation from the torque of the motor to the control force given in Fig.5. The voltage equation for the motor is expressed as follows:

$$L\dot{i} + Ri + K_e\eta = e \quad (4)$$

where e and i indicate the input voltage and the current of the motor respectively. The torque of the motor is given by

$$T_m = K_t i \quad (5)$$

As shown in Fig.5, the torque balance can be expressed as follows:

$$T_n = r_g T_m - (I_m + I_{gm}) r_g \ddot{\eta} - (I_n + I_{gn}) \ddot{\xi} \quad (6)$$

where $\eta = r_g \xi$, $\xi = d_2 x$ and r_g indicate the rotational displacements of motor and nut, and gear ratio respectively. T_n , T_{gm} and T_{gn} indicate the torques of rotary nut, motor side gear pulley and nut side gear pulley respectively. The relationship between the torque of the rotary nut and the control force can be written as follows:

$$F = d_2 T_n \quad (d_2 = 2\pi/l) \quad (7)$$

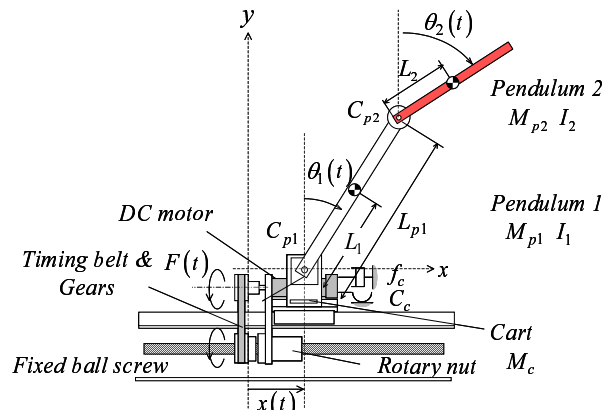


Fig. 4. Model of Double Pendulum on a Cart.

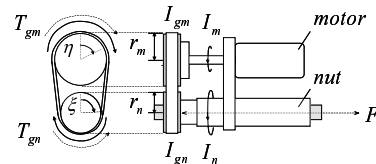


Fig. 5. Translation from Torque of Motor to Control Force.

TABLE I
PHYSICAL PARAMETERS

Symbol	Quantity	Value
M_c	mass of cart	2.824 kg
M_{p1}	mass of pendulum 1	0.264 kg
M_{p2}	mass of pendulum 2	0.054 kg
L_{p1}	length of pendulum 1	0.321 m
L_{p2}	length of pendulum 2	0.194 m
L_1	length from joint to a center of mass of pendulum 1	0.215 m
L_2	length from joint to a center of mass of pendulum 2	0.095 m
I_1	moment of inertia of pendulum 1	$3.22 \times 10^{-3} \text{kg} \cdot \text{m}^2$
I_2	moment of inertia of pendulum 2	$1.86 \times 10^{-4} \text{kg} \cdot \text{m}^2$
I_m	moment of inertia of motor axis	$6.96 \times 10^{-6} \text{kg} \cdot \text{m}^2$
I_n	moment of inertia of rotary nut	$4.80 \times 10^{-5} \text{kg} \cdot \text{m}^2$
I_{gm}	moment of inertia of gear pulley(motor)	$2.20 \times 10^{-6} \text{kg} \cdot \text{m}^2$
I_{gn}	moment of inertia of gear pulley(nut)	$2.56 \times 10^{-5} \text{kg} \cdot \text{m}^2$
f_c	coulomb friction of cart	45 kg · m/s ²
C_c	damping coefficient of cart	177 kg/s
C_{p1}	damping coefficient of pendulum 1	$2.67 \times 10^{-3} \text{kg} \cdot \text{m/s}^2$
C_{p2}	damping coefficient of pendulum 2	$1.02 \times 10^{-4} \text{kg} \cdot \text{m/s}^2$
l	lead of ball screw	$1.60 \times 10^{-2} \text{m/round}$
d_2	transfer coefficient from torque to force	$1.02 \times 10^{-4} \text{kg} \cdot \text{m/s}^2$
L	inductance of motor	$6.20 \times 10^{-4} \text{H}$
R	resistance of motor	2.07 W
K_e	induced voltage constant of motor	$5.25 \times 10^{-2} \text{N} \cdot \text{s/A}$

Introducing Eq. (6) into Eq. (7), we obtain

$$F = \frac{K_t}{R} d_2 r_g e - \frac{K_t K_e}{R} d_2^2 r_g^2 \dot{x} - [(I_m + I_{gm}) r_g^2 + (I_n + I_{gn})] d_2^2 \ddot{x} \quad (8)$$

These dynamical models are nonlinear for the pendulum angle. There is friction between the cart and the fixed ball screw. The physical parameters of experimental equipment are shown in Table I.

IV. DESIGN OF CONTROLLER

The design technique of the proposed method is described as follows. The structure of the proposed integrated intelligent controller is shown in Fig.6. Firstly, three stabilization controllers are designed individually based on linear models around each unstable equilibrium point. Secondly, one swing-up controller is designed based on the energy of the double pendulum. Finally, the integrator neural network is prepared in parallel with these controllers.

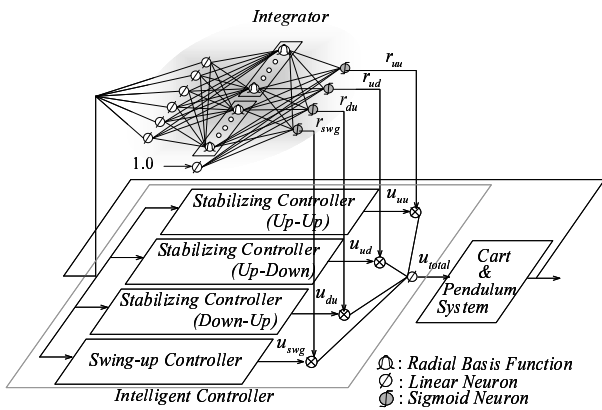


Fig. 6. Structure of Integrated Intelligent Control System.

A. Stabilization Controller

A stabilization controller should stabilize the double pendulum near the unstable equilibrium point. The stabilization controller is realized as a state-space controller with the feedback gain vector \mathbf{k}_i , which is calculated according to the linear-quadratic regulator (LQR) design method. The following control gain vector \mathbf{k}_i and state variables \mathbf{x}_i at each equilibrium point are used.

Down-Up

$$Q_{du} = \text{diag} (0 \ 300 \ 0 \ 1 \ 0 \ 1), R_{du} = 1.0$$

$$\mathbf{k}_{du} = [-85.9198 \ -17.3205 \ 53.2593 \ 493.0170 \ -65.6931 \ -616.7089]$$

$$\mathbf{x}_{du} = [\dot{x} \ x \ \dot{\theta}_{1d} \ \theta_{1d} \ \dot{\theta}_2 \ \theta_2]^T$$

$$u_{du} = -\mathbf{k}_{du} \cdot \mathbf{x}_{du} \quad (9)$$

Up-Down

$$Q_{ud} = \text{diag} (0 \ 300 \ 0 \ 50000 \ 0 \ 500), R_{ud} = 1.0$$

$$\mathbf{k}_{ud} = [-92.3226 \ -17.3205 \ -32.4339 \ -313.7022 \ -0.2756 \ 14.3866]$$

$$\mathbf{x}_{ud} = [\dot{x} \ x \ \dot{\theta}_1 \ \theta_1 \ \dot{\theta}_{2d} \ \theta_{2d}]^T$$

$$u_{ud} = -\mathbf{k}_{ud} \cdot \mathbf{x}_{ud} \quad (10)$$

Up-Up

$$Q_{uu} = \text{diag} (0 \ 300 \ 0 \ 1 \ 0 \ 1), R_{uu} = 1.0$$

$$\mathbf{k}_{uu} = [10.2913 \ 17.3205 \ 14.0202 \ -353.1186 \ -64.2297 \ 607.4820]$$

$$\mathbf{x}_{uu} = [\dot{x} \ x \ \dot{\theta}_1 \ \theta_1 \ \dot{\theta}_2 \ \theta_2]^T$$

$$u_{uu} = -\mathbf{k}_{uu} \cdot \mathbf{x}_{uu} \quad (11)$$

B. Swing-up Controller

A design method based on the energy of the pendulum of the swing-up controller for a rotational pendulum system has been proposed [10]-[13]. The controller design was performed based on the following assumptions: there is no limitation on the velocity of the pendulum and the friction is neglected. However, in practice, there are friction and a physical limitation, especially on the length of the cart track and the magnitude of the control input. Therefore, it is not easy to control the desired acceleration of the cart under the influence of such physical conditions.

In this study, the swing-up controller which takes care of the physical limitations is designed based on the energy of the pendulum. The energy of the uncontrolled double pendulum ($u = 0$) is written as follows:

$$E = \frac{1}{2} (I_1 + M_{p1} L_1^2 + M_{p2} L_{p1}^2) \dot{\theta}_1^2 + M_{p2} L_{p1} L_2 \dot{\theta}_1 \dot{\theta}_2 \cos(\theta_1 - \theta_2) + \frac{1}{2} (I_2 + M_{p2} L_2^2) \dot{\theta}_2^2 + M_{p1} L_1 g (\cos \theta_1 - 1) + M_{p2} g [L_{p1} (\cos \theta_1 - 1) + L_2 (\cos \theta_2 - 1)] \quad (12)$$

The nominal energy is defined to be zero when the double pendulum is in Up-Up equilibrium point. Therefore, the swing-up controller can input enough energy into the system so that it is able to reach the desired equilibrium point from an arbitrary angle of the pendulum.

$$u_{swg} = \alpha \cdot \left\{ \frac{2}{1 + \exp[-\gamma \cdot (E - \beta) \cdot \text{sgn}_x(\theta_1)]} - 1 \right\} \quad (13)$$

$$\text{sgn}_x(\theta_1) = \begin{cases} 1 & : \sin \theta_1 > 0 \text{ or } \sin \theta_1 = 0 \cap x \geq 0 \\ -1 & : \sin \theta_1 < 0 \text{ or } \sin \theta_1 = 0 \cap x < 0 \end{cases} \quad (14)$$

The swing-up controller is specified by three parameters $\{\alpha, \beta, \gamma\}$. α and β indicate the parameters for the limitation of the track length and for compensation of the friction loss of the system respectively. γ represents the parameter of a sigmoid function in order to reduce the chattering. Determination of the values of α , β and γ requires some trial and error and is difficult to do manually. In this study, $\alpha = 16$, $\beta = 0.15$ and $\gamma = 0.15$ are used.

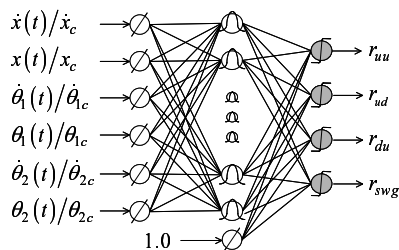
C. Integrator Neural Network

To transfer and stabilize the double pendulum from the arbitrary equilibrium point to the desired unstable one without touching the physical limitations, these designed controllers should be switched and integrated adequately according to the situation. However, it is not easy to derive theoretically suitable switching and integration rules of several controllers. In the method, as shown in Fig.6, the integrator neural network is prepared in parallel with several local controllers. The integrator switches and integrates four controllers automatically and appropriately based on the system states. Since the double pendulum has three unstable equilibrium points, we design three integrators, *integrator_{du}*, *integrator_{ud}* and *integrator_{uu}*, by using the similar architecture of radial basis function neural network and learning method.

1) *Architecture of Integrator*: The architecture of the integrator neural network is shown in Fig.7. The integrator adopts the hidden layers which consist of the following radial basis neurons.

$$\varphi_j(\mathbf{x}, \mathbf{a}_j, \mathbf{b}_j) = \prod_{i=1}^l \exp \left\{ -\frac{(\mathbf{x} - \mathbf{a}_j)^2}{\mathbf{b}_j^2} \right\} \quad (15)$$

where, \mathbf{x} is the input vector with elements x_i , and \mathbf{a}_j is the vector determining the center of basis function φ_j and has elements a_{ji} . \mathbf{b}_j represents the vector determining the width of the Gaussian and has elements b_{ji} . l is the number of nodes in the input layer. The following sharply sigmoid



⊗: Radial Basis Function ⊙: Linear Neuron ⊕: Sharply Sigmoid Neuron

Fig. 7. Integrator Neural Network

function r_k is used as an activation function of the output node k .

$$r_k(\mathbf{x}) = \frac{1}{1 + \exp \left(-200 \left(\sum_{j=1}^m w_{kj} \cdot \varphi_j(\mathbf{x}) + w_{k\theta} \right) \right)} \quad (16)$$

where, w_{kj} is a weight connecting the output node k to the hidden node j and $w_{k\theta}$ is a bias weight. m is the number of nodes in the hidden layer. r_k varies continuously between 0 and 1 and means the degree of importance for each controller. In other words, it can be expected that adjustment of each control gain is performed according to the situation. The control input u_{total} is defined as the following equation.

$$u_{total} = r_{uu}u_{uu} + r_{ud}u_{ud} + r_{du}u_{du} + r_{swg}u_{swg} \quad (17)$$

2) *Learning Method*: The integrator is specified by four adjustable parameters $\{a_{ji}, b_{ji}, w_{kj}, w_{k\theta}\}$. In this study, tuning of them is carried out based on the GA. These parameters are regarded as GA parameters and GAs begin a set of thirty randomly generated states, called the population. During training GA process, (a) initial population, (b) fitness function, (c) selection, (d) crossover and (e) mutation, the individual chromosome to perform the control objective is searched. To calculate the fitness value, the following fitness function is prepared.

$$f_{fit} = \frac{h(x)}{n} \cdot \sum_{t=0}^n \left(\frac{1}{10 \cdot p_1^2(t) + 10 \cdot p_2^2(t) + 1} \right) \quad (18)$$

$$h(x) = \begin{cases} 1 & |x| \leq 0.4 \text{ m} \\ 0.1 & |x| > 0.4 \text{ m} \end{cases} \quad (19)$$

where, $n = t_f / \Delta t$. t_f and Δt represent the simulation period and the sampling period respectively. In this study, $t_f = 10\text{s}$ and $\Delta t = 5\text{ms}$ are used. p_1 and p_2 are set out as shown in Table II. The fitness value is the highest when the double pendulum is in the desired unstable equilibrium point. In our practical facility, the movable track length of the cart is limited. $h(x)$ indicates the penalty function on the cart position limit. When the cart reaches the end of the track, the fitness value is low. In the particular case from Up-Down to Up-Up, the following fitness function in consideration of energy variation is used to swing-up and stabilize the double pendulum without falling down.

$$f_{fit} = \frac{h(x) \cdot k(\theta_1)}{n} \cdot \sum_{t=0}^n \left(\frac{1}{10 \cdot \theta_1^2(t) + 10 \cdot \theta_2^2(t) + 1} \right) \quad (20)$$

$$k(\theta_1) = \begin{cases} 1 & |\theta_1| \leq 0.2 \text{ rad} \\ 0.01 & |\theta_1| > 0.2 \text{ rad} \end{cases} \quad (21)$$

TABLE II
GA PARAMETERS.

desired equilibrium point	p_1	p_2	j_1 : initial states (θ_1, θ_2)		
			$j_1 = 0$	$j_1 = 1$	$j_1 = 2$
Down-Up	θ_{1d}	θ_2	(π, π)	$(0, \pi)$	$(0, 0)$
Up-Down	θ_1	θ_{2d}	(π, π)	$(\pi, 0)$	$(0, 0)$
Up-Up	θ_1	θ_2	(π, π)	$(\pi, 0)$	$(0, \pi)$

where $k(\theta_1)$ indicates the penalty function on the pendulum 1 angle. If once the double pendulum is falling down, the fitness value is low. In the cases from three initial conditions shown in Table II, the above-mentioned fitness function is calculated and then the sum of them is regarded as the fitness value of the individual chromosome.

$$f_{fit_total} = \sum_{j_1=0}^2 f_{fit}(j_1) \quad (22)$$

During training the GA process, one individual chromosome whose fitness value is maximum is chosen as the integrator neural network.

V. EXPERIMENTAL RESULT

In order to verify the performance of the proposed method, simulations for the cases from the arbitrary equilibrium points to each unstable equilibrium point were carried out. From the results, it was confirmed that the proposed controller can achieve all nine paths among equilibrium points by switching and integrating four controllers autonomously and adequately according to situations. In addition, experiments using a real apparatus were carried out. The initial states of \dot{x} , x , $\dot{\theta}_1$ and $\dot{\theta}_2$ are zero. In this study, the length of the track is 0.8m. The servo motor range is $\pm 25V$. The displacement of the cart and the angular displacements of the pendulum 1 and the pendulum 2 are observed at the intervals of 5ms, that is, the sampling period. Their velocities are calculated from the difference between sequential displacements. Figures 8 to 12 show the time histories, in order, the displacement of the cart, the angular displacements of pendulum 1 and pendulum 2, the control input and the outputs of the integrator. Figures 8 to 10 show the result of the experiments when it was initialized at the stable equilibrium point, that is, Down-Down respectively. It was demonstrated as shown in Fig.8 that the controller can transfer the double pendulum from Down-Down by integrating Down-Up with Up-Up stabilization controllers and then stabilize it near Down-Up by switching only the Down-Up stabilization controller. As shown in Figs. 9 and 10, the proposed controller can transfer and stabilize the double pendulum from Down-Down to near the desired unstable equilibrium point respectively. Fig.13(a) shows the view of the double pendulum on a cart during swinging up and stabilizing control for the case that started from Down-Down to Up-Up. Figures 11 and 12 show the result of the experiments for the transfer and stabilization control between two unstable equilibrium points. Figure 11 shows the result of the experiment when it was initialized at Up-Up. It can be seen from Fig.11 that the controller can transfer the double pendulum from the Up-Up to Up-Down without falling down by integrating Up-Down stabilization controller with the swing-up controller and then stabilize it near the Up-Down equilibrium point by switching only Up-Down stabilization controller. It was demonstrated as shown in Figs. 12 and 13(b) that the proposed controller

can transfer and stabilize the double pendulum from Up-Down to Up-Up without falling down by switching and integrating four controllers adequately.

VI. CONCLUSION

In this paper, an effective robust intelligent control method for nonlinear and complicated systems was presented. To cope with the increases of number of controllers and switching rules of several controllers for such systems, the integrator neural network which switches and integrates several controllers based on the system states was proposed.

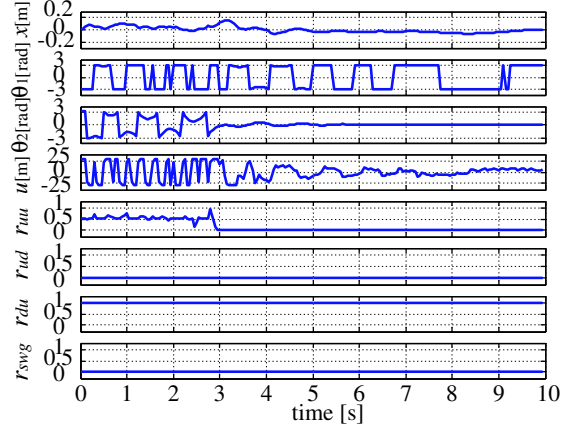


Fig. 8. Experimental Result from Down-Down to Down-Up.

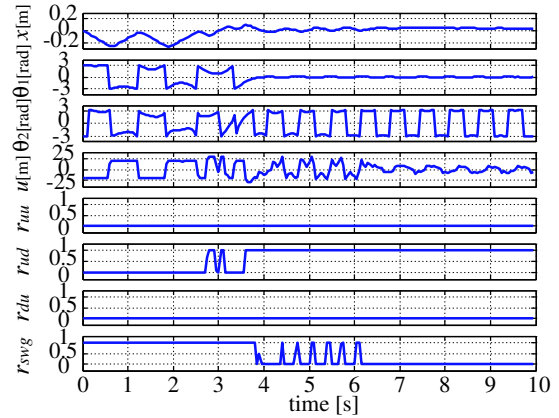


Fig. 9. Experimental Result from Down-Down to Up-Down.

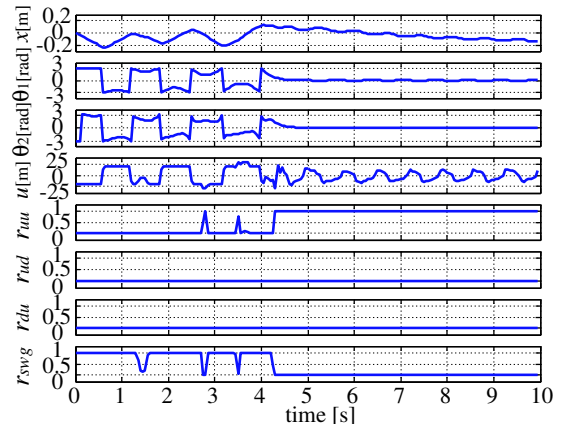


Fig. 10. Experimental Result from Down-Down to Up-Up.

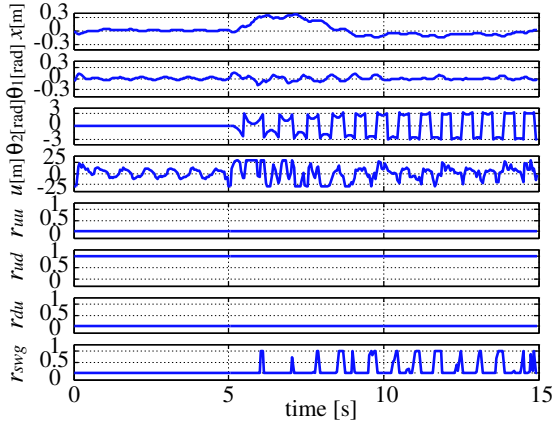


Fig. 11. Experimental Result from Up-Up to Up-Down.

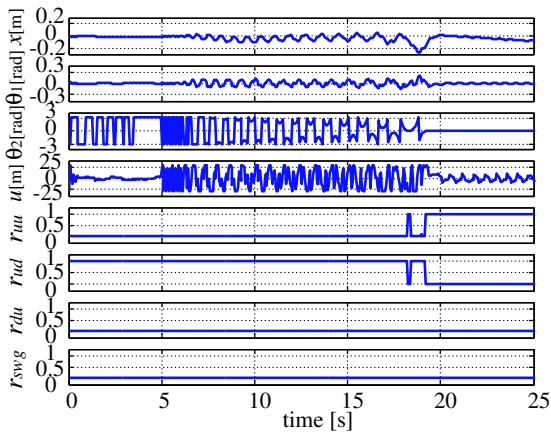
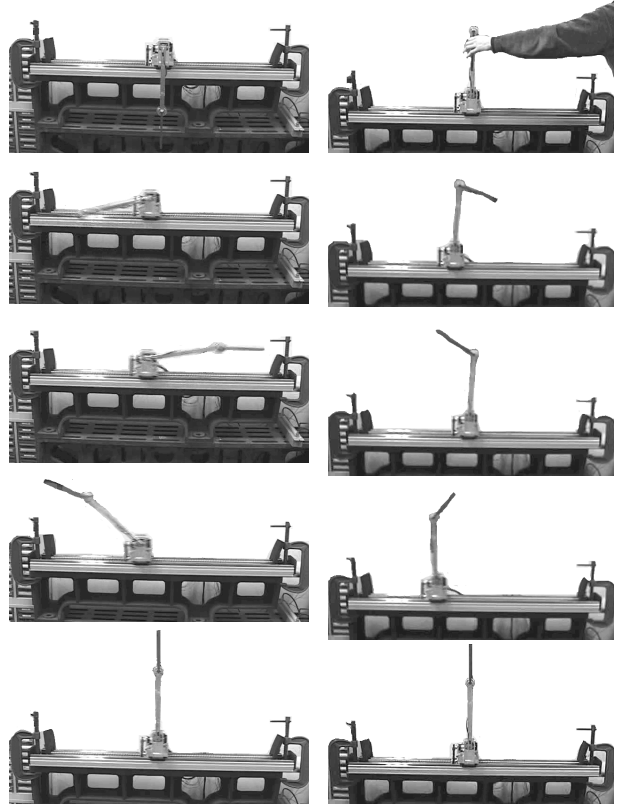


Fig. 12. Experimental Result from Up-Down to Up-Up.

For the application to the equilibrium point transfer and stabilization control of the double pendulum which has four equilibrium points, the integrator which takes consideration into the physical limitations was designed. In order to verify the effectiveness of the proposed method, computational simulations and experiments on a real facility were carried out. As a result, it was confirmed that the proposed controller can transfer and stabilize the double pendulum from the arbitrary equilibrium point to the desired unstable one. From the simulations and the experiments, it was demonstrated that the integrated intelligent control method is useful for nonlinear and complicated systems.

REFERENCES

- [1] M. Yamakita, K. Nonaka and K. Furuta, Swing Up Control of Double Pendulum, *Proc. ACC'93*, 1993, pp 2229-2234.
- [2] S. Mori, H. Nishihara and K. Furuta, Control of Unstable Mechanical System Control of Pendulum, *Int. J. Control*, vol. 23, no. 5, 1976, pp 673-692.
- [3] E. P. Dadios and D. J. Williams, Nonconventional Control of the Flexible Pole-Cart Balancing Problem: Experimental Results, *IEEE Trans. Systems, Man and Cybernetics*, vol. 28, no. 6, 1998, pp 895-901.
- [4] K. Yoshida and K. Hatano, Intelligent Control Using Cubic Neural Network for Swinging up and Stabilizing Pendulum, *Int. J. JSME*, vol. 43, no. 3, 2000, pp 612-617.



(a) From Down-Down to Up-Up. (b) From Up-Down to Up-Up.

Fig. 13. Experimental Result.

- [5] K. Furuta, H. Kajiwara and K. Kosuge, Digital Control of a Double Inverted Pendulum on an Inclined Rail, *Int. J. Control*, vol. 32, no. 5, 1980, pp 907-924.
- [6] J. Rubí, A. Rubio and A. Avello, Swing-up Control Problem for a Self-erecting Double Inverted Pendulum, *IEE Proc. Control Theory and Applications*, vol. 149, no. 2, 2002, pp 169-175.
- [7] M. Takahashi and K. Yoshida, Intelligent Failure-Proof Control using Cubic Neural Network (Application to Swinging up and Stabilizing Double Pendulum), *Proc. Motion and Vibration Control*, no. 02-201, 2002, pp 265-270.
- [8] M. Yamakita, M. Iwashiro, Y. Sugahara and K. Furuta, Robust Swing Up Control of Double Pendulum, *Proc. ACC 95*, 1995, pp 290-295.
- [9] M. Yamakita and K. Furuta, Toward Robust State Transfer Control of TITech Double Pendulum, *The Astrom Symposium on Control*, ed. B. Wittenmark and A. Rantzer, Studentlitteratur, 1999, pp 73-96.
- [10] M. Wiklund, A. Kristenson and K. J. Åström, A New Strategy For Swinging Up An Inverted Pendulum, *Proc. The 12th Triennial World Congress of the International Federation of Automatic Control*, 1993, pp 757-760.
- [11] W. Zhong and H. Röck: Energy and Passive Based Control of the Double Inverted Pendulum on a Cart, *Proc. IEEE, Int. Conf. Control Applications*, 896/901 (2001).
- [12] K. J. Åström and K. Furuta, Swinging Up a Pendulum by Energy Control, *Automatica*, vol. 36, no. 2, 2000, pp 287-295.
- [13] D. Chatterjee, A. Prtra and H. K. Joglekar, Swing-up and stabilization of a cart-pendulum system under restricted cart track length, *System and Control Letters*, vol. 47, 2002, pp 355-364.

VII. ACKNOWLEDGMENTS

This work is supported in part by Grant in Aid for the 21st century center of Excellence for "System Design : Paradigm Shift from Intelligence to Life" from Ministry of Education, Culture, Sport, and Technology in Japan.